Hypersensitivity to mGluR5 and ERK1/2 Leads to Excessive Protein Synthesis in the Hippocampus of a Mouse Model of Fragile X Syndrome

Published in final edited form as:
J Neurosci. 2010 November 17; 30(46): 15616–15627. doi:10.1523/JNEUROSCI.3888-10.2010.

Hypersensitivity to mGluR5 and ERK1/2 leads to excessive protein synthesis in the hippocampus of a mouse model of fragile X syndrome

Emily K. Osterweil, **Dilja D. Krueger**, **Kimberly Reinhold**, and **Mark F. Bear**
Howard Hughes Medical Institute, Picower Institute for learning and Memory, Department of Brain and Cognitive Sciences, Massachusetts Institute of Technology, Cambridge, MA

Abstract

Fragile X syndrome (FXS) is caused by loss of the *FMR1* gene product FMRP, a repressor of mRNA translation. According to the mGluR theory of FXS, excessive protein synthesis downstream of metabotropic glutamate receptor 5 (mGluR5) activation causes the synaptic pathophysiology that underlies multiple aspects of fragile X syndrome (FXS). Here, we utilize an *in vitro* assay of protein synthesis in the hippocampus of male *Fmr1* KO mice to explore the molecular mechanisms involved in this core biochemical phenotype under conditions where aberrant synaptic physiology has been observed. We find that elevated basal protein synthesis in *Fmr1* KO mice is selectively reduced to wild type (WT) levels by acute inhibition of mGluR5 or ERK1/2, but not by inhibition of mTOR. The mGluR5-ERK1/2 pathway is not constitutively overactive in the *Fmr1* KO, however, suggesting that mRNA translation is hypersensitive to basal ERK1/2 activation in the absence of FMRP. We find that hypersensitivity to ERK1/2 pathway activation also contributes to audiogenic seizure susceptibility in the *Fmr1* KO. These results suggest that the ERK1/2 pathway, and other neurotransmitter systems that stimulate protein synthesis via ERK1/2, represent additional therapeutic targets for FXS.

Keywords

fragile X; mGluR5; mGluR-LTD; ERK; mTOR; protein synthesis; FMRP

Introduction

Fragile X syndrome (FXS) is caused by the loss of the *FMR1* gene product FMRP (Verkerk et al., 1991). Converging lines of evidence suggest that FMRP represses mRNA translation in neurons and that cerebral protein synthesis is elevated in the absence of FMRP (Laggerbauer et al., 2001; Li et al., 2001; Huber et al., 2002; Aschrafi et al., 2005; Qin et al., 2005; Dolen et al., 2007; Bolduc et al., 2008). Group 1 (Gp1) metabotropic glutamate receptors (mGluR1 and mGluR5) stimulate mRNA translation at synapses (Weiler and Greenough, 1993; Weiler et al., 1997) and many lasting physiological consequences of Gp1 mGluR activation require rapid synaptic protein synthesis (Merlin et al., 1998; Huber et al., 2000; Raymond et al., 2000; Karachot et al., 2001; Vanderklish and Edelman, 2002; Banko et al., 2006). Based initially on the finding that mGluR-dependent long-term synaptic depression (mGluR-LTD) is exaggerated in the hippocampus of *Fmr1* knockout (KO) mice (Huber et al., 2002), the proposal was made that many of the symptoms of FXS might

Corresponding author: Mark F. Bear, The Picower Institute for Learning and Memory, MIT 46-3301, 43 Vassar Street, Cambridge, MA 02139, mbear@mit.edu.

plausibly be explained by excessive protein synthesis downstream of Gp1 mGluR activation (Bear et al., 2004). The prediction that multiple aspects of fragile X can be corrected by reducing or inhibiting mGluR5 has been confirmed in numerous studies in several species (reviewed by Dolen and Bear, 2008).

Although it is now clear that mGluR5 participates in the pathogenesis of FXS, at least in animal models, it is still poorly understood how Gp1 mGluRs trigger protein synthesis and how this process is altered in the absence of FMRP to disrupt synaptic function. Several studies have examined this issue in the hippocampus and cortex, but no clear consensus has emerged (Weiler et al., 2004; Hou et al., 2006; Muddashetty et al., 2007; Kim et al., 2008; Park et al., 2008; Ronesi and Huber, 2008; Sharma et al., 2010). One source of confusion may be that proxy measures of protein synthesis, such as mGluR-LTD or phosphorylation of signaling molecules, have been used in intact hippocampal slice preparations, whereas metabolic labeling experiments have been performed in synaptoneurosome preparations of cortex that are not easily related to altered hippocampal synaptic plasticity.

In the current study, we reexamine the question of how protein synthesis is elevated in the *Fmr1* KO using a metabolic labeling approach in hippocampal slices maintained under the same conditions that revealed altered mGluR-dependent synaptic plasticity in previous studies from our laboratory (Huber et al., 2002; Auerbach and Bear, 2010). A strong rationale for taking this approach is that slice has been shown to accurately reproduce the *in vivo* phenotype of elevated basal protein synthesis in the *Fmr1* KO hippocampus (*cf.* Qin et al., 2005; Dolen et al., 2007). Further, besides reproducing this core biochemical phenotype, the slice has the advantage that it enables pharmacological and biochemical access that is not possible *in vivo*. Our data suggest that elevated protein synthesis in the *Fmr1* KO is due to saturation of mRNA translation downstream of the MAP kinase ERK1/2 which is basally activated by mGluR5.

Materials and Methods

Mice

Fmr1 KO (Jackson Labs) and wild type littermates were kept on the C57Bl/6J background, group housed, and maintained in a 12:12 h light:dark cycle. All animals were treated in accordance with NIH and MIT guidelines. All experiments were performed blind to genotype. On each day of slice experimentation, 4 animals from each genotype were sacrificed in an interleaved fashion and slices were prepared as rapidly as possible (≤ 5 min) as described below. This procedure yielded yoked, same-day controls for genotype and drug treatments.

Drugs

(R,S)-3,5-Dihydroxyphenylglycine (DHPG), 2-Methyl-6-(phenylethynyl)pyridine hydrochloride (MPEP), 1,4-Diamino-2,3-dicyano-1,4-bis[2-aminophenylthio]butadiene (U0126), actinomycin D (ActD), and a-[Amino[(4-aminophenyl)thio]methylene]-2-(trifluoromet hyl)benzeneacetonitrile (SL 327) were obtained from Tocris Bioscience. DHPG and MPEP stocks were freshly prepared in ddH_2O on the day of the experiment. ActD stock was prepared in ACSF + 0.5% DMSO and kept at −20°C. Anti-TrkB (R&D Systems), BDNF (Peprotech), insulin (Sigma), rapamycin (EMD Biosciences), cycloheximide (EMD Biosciences), U0126, and SL 327 were reconstituted according to manufacturer's instructions and either used immediately or stored at −20°C. For all slice experiments, the final concentration of DMSO was less than 0.1%.

Metabolic labeling

Juvenile (P25–P30) male littermate WT and *Fmr1* KO mice were given an overdose of Nembutal, and the hippocampus rapidly dissected into ice-cold artificial cerebral spinal fluid (ACSF) (in mM: NaCl: 124, KCl: 3, NaH_2PO_4: 1.25, $NaHCO_3$: 26, dextrose: 10, $MgCl_2$: 1, $CaCl_2$: 2, saturated with 95% O_2 and 5% CO_2). Slices (500 μm thick) were prepared using a Stoelting Tissue Slicer, and transferred into 32.5°C ACSF (saturated with 95% O_2 and 5% CO_2) within 5 min. Unless indicated otherwise, slices were incubated in ACSF undisturbed for 3.5–4 h to allow for recovery of protein synthesis (Sajikumar et al., 2005). 25 μM ActD was then added to the recovery chamber for 30 min to inhibit transcription. For DHPG (100 μM) and whole-slice MPEP (50 μM) experiments, slices were incubated in 10 μCi/ml ^{35}S-Met/Cys (express protein labeling mix, Perkin Elmer) ± drug for 5 min, and transferred to fresh ACSF with 10 μCi/ml ^{35}S-Met/Cys for another 25 min to measure protein synthesis. For cycloheximide (60 μM; performed in WT), CA1 MPEP (10 μM), U0126 (5 μM), and rapamycin (20 nM) experiments, slices were incubated ± drug during ActD exposure (30 min), and transferred to fresh ACSF with 10 μCi/ml ^{35}S-Met/Cys ± drug for another 30 min. For TrkB activation experiments, slices were incubated ± 1 μg/ml anti-TrkB for 30 min, then 25 μM ActD ± 1 μg/ml anti-TrkB for 30 min, and protein synthesis measured with 10 μCi/ml ^{35}S-Met/Cys ± 1 μg/ml anti-TrkB for 1 h. After labeling, slices were either snap frozen in liquid nitrogen or processed immediately.

With the exception of CA1 MPEP experiments, slices were homogenized in ice-cold homogenization buffer (10 mM HEPES pH 7.4, 2 mM EDTA, 2 mM EGTA, 1% Triton X-100, protease inhibitors (cocktail III, EMD Biosciences), and phosphatase inhibitors (cocktails I + II, EMD Biosciences)), and incubated in trichloroacetic acid (TCA; 10% final) for 10 min on ice to precipitate radiolabeled proteins. Samples were then spun at 21,000×g for 10 min, and the pellet washed with ice-cold ddH_2O and resuspended in 1 N NaOH until dissolved. After adjustment to a neutral pH with HCl, triplicate aliquots of each sample were added to scintillation cocktail (HiSafe II, Perkin Elmer) and read with a scintillation counter, and also subjected to a protein concentration assay (Bio-Rad). Averaged triplicate counts per minute (CPM) values were divided by protein concentrations, resulting in CPM per μg protein. To control for daily variation in incorporation rate, the values obtained on each day were normalized to the ^{35}S-Met/Cys ACSF used for incubation, and the average incorporation of all slices analyzed in that experiment, as described by Lipton and Raley-Susman (1999).

For CA1-MPEP experiments, slices were briefly thawed and CA1 regions were dissected. To obtain autoradiographs, aliquots of homogenized CA1 were taken prior to TCA precipitation and boiled in Laemmli sample buffer. Samples were then resolved on SDS PAGE gels, transferred to nitrocellulose, and stained for total protein (Memcode staining kit, Pierce). Blots were exposed to a phosphorimager screen for 24–72 hours, and the screen read with a phosphorimager (Fujifilm). To quantify autoradiographs and Memcode-stained blots, a line-scan of each lane was measured and quantified using the gel analyzer tool in Image J. Protein synthesis was calculated by normalizing data from autoradiographs to Memcode staining data obtained from the same lanes.

Acute stimulation

Slices were prepared and allowed to recover as for metabolic labeling, incubated in 100 μM DHPG for exactly 5 min or 1 μM insulin for 10 min, then snap frozen in liquid nitrogen. Frozen slices were either immediately homogenized in Laemmli sample buffer containing phosphatase inhibitors, or briefly thawed and microdissected in homogenization buffer with protease and phosphatase inhibitors (minus detergent). Microdissected regions were

homogenized in sample buffer containing phosphatase inhibitors immediately following dissection.

Synaptoneurosomes

Synaptoneurosomes were isolated from sets of 4 slices essentially as described previously (Chen and Bear, 2007). Slices were homogenized on ice using 2 ml glass dounces (Wheaton), passed through 2 × 105 μm meshes, followed by 1 × 5 μm mesh, and the resulting samples spun at 1,000 × g for 10 min at 4°C. Pellets were washed, spun at 1,000 × g, and processed for SDS PAGE.

Immunoblotting

Samples were boiled in Laemmli sample buffer, resolved on SDS PAGE gels, transferred to nitrocellulose, and stained for total protein. Immunoblotting was performed with the following primary antibodies: from Cell Signaling Technology: p-ERK1/2 (Thr202/Tyr204), ERK1/2, p-p38 (Thr180/Tyr182), p38, p-Akt (Ser473), p-mTOR (Ser2448), mTOR, p-PTEN (Ser380/Thr382/383), PTEN, p-p70S6K (Thr389), p70S6K, p-S6 (Ser235/236), S6 p-Trk (Tyr490), and GAPDH; other: TrkB (BD Biosciences), and alpha-CaMKII (Sigma). After incubation in primary antibody overnight at 4°C, immunoblots were either incubated with fluorophore-conjugated secondary antibodies and imaged with the Odyssey imaging system (LiCor Biosciences), or incubated with HRP-conjugated secondary antibodies (GE Healthcare), developed with ECL plus (GE Healthcare) and exposed to film. Densitometry was performed on scanned blot films or LiCor images using Quantity One software (Bio-Rad). Data were expressed as the value of the phosphorylation signal divided by the value of the total protein signal in the same lane. To correct for blot-to-blot variance, each signal was normalized to the average signal of all lanes on the same blot. All gels were loaded and analyzed blind to genotype and treatment.

Fresh dissections

WT and *Fmr1* KO (P25–32) male littermates were sacrificed by rapid decapitation, and hippocampi rapidly dissected into ice-cold homogenization buffer. Tissue was homogenized on ice using 2 ml glass dounces, and processed for SDS PAGE.

Immunoprecipitation

Hippocampal slices (5–8 per animal) were prepared as described above from WT and *Fmr1* KO mice and metabolically labeled with 50 μCi/ml ^{35}S-Met/Cys for 1 h in order to ensure visualization of individual target proteins. Immunoprecipitation (IP) experiments were performed on yoked WT and *Fmr1* KO slices essentially as described in Osterweil et al. (2005) and Kundel et al. (2009). Briefly, slices were homogenized in ice-cold homogenization buffer with 200 mM NaCl, spun at 2,000 × g for 5 min, and the supernatant adjusted to 400 mM NaCl. Samples were then spun at 16,000 × g for 30 min, pre-cleared with 1/10 volume protein-A-sepharose (GE Healthcare) for 1 hour at 4°C, and incubated 10 μg/ml non-immune mouse IgG (Santa Cruz), mouse anti-GAPDH (Millipore), or mouse anti-alpha-CaMKII (Millipore) overnight at 4°C. Samples were then incubated with 1/10 volume protein-A-sepharose for 2 h at 4°C, and the IPs washed 5 × 1 ml homogenization buffer with 400 mM NaCl. IPs were resuspended in an equal volume Laemmli sample buffer, resolved on SDS PAGE gels, transferred to nitrocellulose, and exposed to a phosphorimager screen for 2–3 weeks. The same membranes were then immunoblotted for alpha-CaMKII and GAPDH. For each sample, the ratio of ^{35}S-incorporated : total was calculated by dividing the density of the band seen by autoradiography to the density of band seen by immunoblot (in the same lane). Experiments were performed and analyzed blind to genotype.

TrkB stimulation

Hippocampal neurons were prepared from E18 rat embryos as described (Krueger and Nairn, 2007), and cultured for 21 days. 30 min prior to stimulation, the medium was removed and replaced with 0.75 ml medium (50% conditioned, 50% fresh) to control for volume. TrkB stimulation was performed with a 15 min incubation of vehicle or 1 μg/ml anti-TrkB, followed by application of vehicle or 100 ng/ml BDNF for 5 min. Plates were then washed with ice-cold PBS, and cells lysed in buffer containing 50 mM Tris, pH 7.4, 1 mM EDTA, 1 mM EGTA, 1% SDS, protease inhibitors and phosphatase inhibitors. Whole-cell lysates were processed for SDS PAGE and immunoblotted.

Audiogenic seizures (AGS)

Experiments were performed essentially as described previously (Dolen et al., 2007). Male WT and *Fmr1* KO littermates (P18–22) were injected intraperitoneally (i.p.) with SL 327 (100 mg/kg; dose based on Zhong et al., 2009), rapamycin (6 mg/kg; dose based on Ehninger et al., 2008 and Meikle et al., 2008) or an equal volume of vehicle (50% DMSO in ddH_2O for SL 327 experiments; 100% DMSO for rapamycin experiments), and returned to their home cage for 1 hour. Each testing session contained at least one set of vehicle-treated controls from each genotype. Mice were then transferred to a transparent plastic test chamber and, after at least 1 minute of habituation, exposed to an alarm (modified personal alarm, 125 dB Radioshack model 49–1010 or 130 dB Samfe model SWPDAL-130, powered from a DC converter) for 2 minutes. For each group, incidence of the following stages of AGS was calculated: wild running, clonic seizure, tonic seizure, and death. All mice were injected and scored blind to genotype.

Statistics

For AGS experiments, significance was determined using two-tailed Fisher's exact test (appropriate for analyzing nominal data sets). For recovery time-course experiments, significance was determined using repeated-measures ANOVA, followed by *post hoc* two-tailed unpaired Student's t-tests. For all other experiments, outliers (± 2 standard deviations from the mean) were removed, and significance between more than two groups was determined by two-way repeated measures mixed model ANOVA. If significant effects were found by ANOVA, *post hoc* analyses were performed to compare individual groups using two-tailed paired Student's t-tests. For data sets that contained only two groups, significance was determined by two-tailed paired Student's t-tests.

Results

Basal protein synthesis is elevated in *Fmr1* KO hippocampus

The molecular mechanisms underlying dysfunctional protein synthesis in the *Fmr1* KO are largely unknown. To explore this question, we employed an *in vitro* assay designed to measure protein synthesis in acute hippocampal slices. In order to directly relate our observations to the aberrant physiology seen in the *Fmr1* KO, we examined slices isolated from P (postnatal day) 25–30 dorsal hippocampus, as this is when and where exaggerated mGluR- and protein synthesis-dependent LTD is observed (Huber et al., 2002). Slices were prepared from dorsal hippocampus, and immediately transferred to 32.5°C ACSF (see Materials and Methods). These slices were then exposed to actinomycin D (ActD, 25 μM) for 30 minutes to prevent new transcription, and protein synthesis was measured over 30 minutes via incorporation of a ^{35}S-labeled methionine/cysteine mix (10 μCi/ml ^{35}S-Met/Cys). To verify that our measurements accurately reflect global protein synthesis, slices were incubated ± 60 μM cycloheximide for 30 minutes, and protein synthesis measured ± 60 μM cycloheximide for an additional 30 minutes. This experiment confirmed that exposure to

cycloheximide, a potent inhibitor of mRNA translation, completely eliminates ^{35}S-Met/Cys incorporation (Figure S1).

A number of previous studies suggest that a long (> 2–4 hour) post-slicing recovery period is necessary to achieve stability in metabolic function (i.e., ATP and creatine levels (Whittingham et al., 1984), signaling cascades (Ho et al., 2004), dendritic spine density (Kirov et al., 1999), and protein synthesis-dependent synaptic plasticity (Huber et al., 2001; Sajikumar et al., 2005). We confirmed and extended this conclusion using our assay of basal protein synthesis in hippocampal slices. We found that optimal and stable protein synthesis recovers 4–6 hours after preparing slices (protein synthesis expressed as % ± SEM of 4 hr value: 0.5 h 76 ± 7%; 1 h 72 ± 8%; 2 h 88 ± 9%; 4 h 100 ± 8%; 6 h 99 ± 8%; ANOVA time $p < 0.05$; n = 10; Figure 1A). This observation is consistent with electrophysiological measurements of optimal protein synthesis-dependent synaptic plasticity in the hippocampus (Sajikumar et al., 2005), including optimal mGluR-LTD (Huber et al., 2001). Therefore for all experiments reported here, the hippocampus was allowed to recover for at least 4 hours following slicing.

To examine whether protein synthesis is elevated in *Fmr1* KO hippocampus under conditions where exaggerated mGluR-LTD is observed, we performed metabolic labeling on juvenile, dorsal *Fmr1* KO slices. Our results reveal a significant elevation of basal protein synthesis in *Fmr1* KO hippocampus as compared to wild type (WT) controls (WT 100 ± 3%, KO 119 ± 5%; t-test $p < 0.02$; n = 13; Figure 1B). The magnitude of this increase in protein synthesis is in quantitative agreement with *in vivo* measurements (Qin et al., 2005), and with our previous results in adult, ventral hippocampus (Dolen et al., 2007).

Autoradiographs of *Fmr1* KO versus WT slices show an increased ^{35}S-Met/Cys incorporation into proteins of multiple molecular weights, which supports the proposal that FMRP functions as a rather general repressor of translation (Figure 1B) (Laggerbauer et al., 2001; Li et al., 2001; Mazroui et al., 2002; Aschrafi et al., 2005). To confirm that our measurement of increased total protein synthesis reflects de-repression of FMRP-regulated translation, we performed immunoprecipitation (IP) experiments to isolate newly made alpha-Ca^{2+}/calmodulin-dependent kinase kinase II (alpha-CaMKII), a validated target mRNA for FMRP (Brown et al., 2001; Zalfa et al., 2003; Ferrari et al., 2007; Muddashetty et al., 2007). Alpha-CaMKII was immunoprecipitated from WT and *Fmr1* KO slices that had been metabolically labeled with 50 μCi/ml ^{35}S-Met/Cys for 1 hour (see Materials and Methods). To ensure the efficacy of our IP experiments, we quantified the amount of alpha-CaMKII (assessed by immunoblot) observed in anti-alpha-CaMKII IPs versus IgG IPs from the same lysates (Figure S2A). Our results confirm that alpha-CaMKII is significantly enriched in the anti-alpha-CaMKII IPs from both WT and *Fmr1* KO slices (WT IgG 100 ± 12%, WT CaMK 600 ± 73%, KO IgG 70 ± 25%, KO CaMK 544 ± 45%; t-test WT IgG vs. CaMK *$p < 0.002$, t-test KO IgG vs. CaMK *$p < 0.0001$; n = 6; Figure S2A). To quantify newly translated protein, ^{35}S-incorporated alpha-CaMKII was measured by autoradiography, and normalized to total alpha-CaMKII in the same IP (Figure 1C). A comparison of these values in WT versus *Fmr1* KO reveals that alpha-CaMKII is excessively translated in hippocampal slices from the *Fmr1* KO (WT 100 ± 12%, KO 124 ± 11%; t-test *$p < 04$; n = 6; Figure 1D). This increase in newly translated alpha-CaMKII is similar in magnitude to the increase seen in total protein synthesis (Figure 1B).

We also performed the same IP experiments for glyceraldehyde phosphate dehydrogenase (GAPDH), a non-FMRP target (Brown et al., 2001). Analysis of GAPDH levels confirmed a significant enrichment in anti-GAPDH IPs versus IgG IPs in both WT and *Fmr1* KO slices (WT IgG 100 ± 19%, WT GAPDH 1832 ± 268%, KO IgG 99 ± 26%, KO GAPDH 2250 ± 314%; t-test WT IgG vs. GAPDH *$p < 0.003$, t-test KO IgG vs. GAPDH *$p < 0.002$; n = 5;

Figure S2B). However, a comparison of ^{35}S-incorporated : total ratios reveals that GAPDH is not excessively translated in *Fmr1* KO slices (WT 100 ± 9%, KO 88 ± 6%; t-test $p = 0.31$; $n = 5$; Figure 1D). These findings suggest that the elevated total protein synthesis we detect in the *Fmr1* KO reflects de-repression of FMRP-regulated translation.

Excessive protein synthesis in the *Fmr1* KO is corrected by acute, pharmacological antagonism of mGluR5

To see whether acute pharmacological inhibition of mGluR5 could effectively reduce the excess protein synthesis seen in juvenile *Fmr1* KO hippocampus, we exposed slices to the mGluR5 antagonist, MPEP. Interestingly, our initial experiments revealed that a 5 minute application of 50 μM MPEP, which had no significant effect on WT protein synthesis, was sufficient to reduce the protein synthesis in *Fmr1* KO slices back to WT levels (WT control 100 ± 1%, KO control 117 ± 2%, WT MPEP 104 ± 2%, KO MPEP 95 ± 2%; ANOVA genotype × treatment $p < 0.05$; $n = 8$; Figure 1E). Because we are particularly interested in the protein synthesis related to mGluR-LTD, we repeated the experiment using an MPEP treatment that has been shown to block LTD (Hou and Klann, 2004) and measured changes in protein synthesis specifically in the CA1 region of dorsal hippocampus. Slices were pre-incubated ± 10 μM MPEP for 30 minutes, then protein synthesis was measured for another 30 minutes ± 10 μM MPEP. Measurements restricted to microdissected area CA1 showed that although MPEP had no effect on protein synthesis under basal conditions in WT slices, it was sufficient to correct elevated protein synthesis in *Fmr1* KO slices (WT control 100 ± 4%, KO control 117 ± 6%, WT MPEP 107 ± 7%, KO MPEP 104 ± 6%; ANOVA genotype × treatment $p < 0.02$; $n = 8$; Figure 1F). These data represent the first demonstration that excessive protein synthesis in the *Fmr1* KO hippocampus can be rapidly corrected by acute pharmacological inhibition of mGluR5. Thus, the elevated protein synthesis in the *Fmr1* KO is downstream of constitutive mGluR5 activation.

mGluR-mediated protein synthesis is mimicked and occluded in the *Fmr1* KO

In hippocampal slices from *Fmr1* KO mice, LTD induced by application of DHPG is greater in magnitude (Huber et al., 2002) and qualitatively unlike WT because it is not reduced by protein synthesis inhibitors (Hou et al., 2006; Nosyreva and Huber, 2006). These findings have led to the suggestion that proteins responsible for long-term expression of LTD are rapidly synthesized in response to mGluR activation in WT, and constitutively over-expressed in *Fmr1* KO hippocampus. Gp1 mGluR activation has been shown to lead to increased protein synthesis in a variety of systems (Weiler and Greenough, 1993; Raymond et al., 2000; Job and Eberwine, 2001; Todd et al., 2003; Shin et al., 2004; Muddashetty et al., 2007). However, whether activation of mGluRs under LTD conditions leads to an increase in protein synthesis in hippocampal slice has not been directly tested.

We observed that the same treatment that induces LTD in hippocampal slices (100 μM DHPG, 5 min) also significantly increases protein synthesis in WT slices (Figure 1G). Interestingly, however, the same treatment does not stimulate protein synthesis over the elevated baseline level in *Fmr1* KO hippocampal slices (WT control 100 ± 2%, WT DHPG 119 ± 2%, KO control 110 ± 5%, KO DHPG 112 ± 4%; ANOVA genotype × treatment $p < 0.02$; $n = 8$; Figure 1G). Thus, genetic deletion of FMRP appears to mimic and occlude the effect of DHPG on protein synthesis.

No detectable difference in basal mGluR signaling under conditions of elevated protein synthesis

Previous studies have shown that DHPG stimulation leads to activation of the MAPK/ERK1/2 pathway (Ferraguti et al., 1999; Gallagher et al., 2004; Hou and Klann, 2004). More recently, activation of the PI3K-Akt-mammalian target of rapamycin (mTOR) pathway has

been reported (Hou and Klann, 2004; Sharma et al., 2010). Both pathways are linked to the initiation of 5' cap-dependent translation of mRNAs (Figure 2A). ERK1/2 activates the MAPK-interacting kinase (Mnk), which leads to phosphorylation of eukaryotic initiation factor 4E (eIF4E) (Proud, 2007). Akt facilitates the activation of mTOR, which de-represses eIF4E by phosphorylating eIF4E binding proteins (4EBPs) (Gingras et al., 1999). mTOR also initiates translation of 5' TOP mRNA, which is linked to the activation of ribosomal protein S6 kinases (i.e., p70S6K), and the subsequent phosphorylation of S6 (Proud, 2007). Phosphorylation of both 4EBP and p70S6K are considered to be reliable and equivalent read-outs of mTOR activation (Hara et al., 1998; Avruch et al., 2001; Wang et al., 2005).

Our results showing that the excessive protein synthesis in the *Fmr1* KO hippocampus is reversible with MPEP application suggest one of two things: (1) mGluR5 signaling is excessive in the *Fmr1* KO hippocampus, or (2) the *Fmr1* KO hippocampus is hypersensitive to normal constitutive mGluR5 signaling. In an attempt to differentiate between these two options, we measured ERK1/2, p38 MAPK, and Akt activation in the same hippocampal slices from WT and *Fmr1* KO that had been used to measure protein synthesis. Interestingly, we observed no basal increase in either ERK1/2 or Akt activation in *Fmr1* KO slices (ERK1/2: WT 100 ± 6%, KO 92 ± 7%; t-test $p = 0.22$; Akt: WT 100 ± 6%, KO 92 ± 4%; t-test $p = 0.12$; $n = 27$; Figure 2B), despite detecting the robust increase in protein synthesis (Figure 1B). There was, however, a small but significant decrease in phosphorylated p38 in the *Fmr1* KO (t-test $*p < 0.05$; $n = 10$; Table 1). This difference may reflect a compensatory downregulation in response to elevated protein synthesis, but is unlikely to be a cause of the increased protein synthesis.

To determine whether upstream or downstream effectors of these pathways were hyperactive, we examined the phosphorylation states of PTEN, a negative regulator of the PI3K pathway (Stambolic et al., 1998), as well as of the downstream components mTOR, p70S6K, and S6. In all proteins tested, no significant increase in activation state was observed in *Fmr1* KO hippocampus (Table 1).

Evoked mGluR-ERK1/2 signaling appears normal in the *Fmr1* KO

Results from untreated slices suggested that basal mGluR5 signaling is not excessive in the *Fmr1* KO hippocampus. However, we could not exclude the possibility that we were missing a change that can only be seen with mGluR5 activation or in a specific biochemical fraction. We therefore measured activation of these pathways after 5 minutes of stimulation with 100 μM DHPG, the protocol for mGluR-LTD induction. Our results revealed that there were no significant differences in activation of ERK1/2, p38, PTEN, Akt, mTOR, p70S6K, or S6 between WT and *Fmr1* KO (Table 2). Interestingly, while we observed a robust activation of ERK1/2 in both WT and *Fmr1* KO slices (WT control 100 ± 6%, WT DHPG 132 ± 8%, KO control 90 ± 6%, KO DHPG 135 ± 6%; ANOVA treatment $p < 0.0001$; $n = 13$; Figure 2C) we did not observe a significant activation of Akt in these slices (WT control 100 ± 5%, WT DHPG 104 ± 6%, KO control 100 ± 5%, KO DHPG 100 ± 6%; ANOVA treatment $p = 0.57$; $n = 14$; Figure 2C). Further investigation revealed that none of the PI3K pathway members examined (PTEN, mTOR, p70S6K and S6) were activated by DHPG in either WT or *Fmr1* KO slices (Table 2).

The exaggerated mGluR-LTD phenotype in *Fmr1* KO has been described in CA1 (Huber et al., 2002), and we wanted to confirm our results in this area of the hippocampus. Consistent with results from whole slices, we found no hyperactivation of ERK1/2 or Akt in area CA1 microdissected from *Fmr1* KO hippocampus, nor was there any occlusion of an mGluR-stimulated response (ERK1/2: WT control 100 ± 3%, WT DHPG 164 ± 6%, KO control 79 ± 7%, KO DHPG 145 ± 16%; ANOVA treatment $p < 0.0001$, genotype × treatment $p = 0.95$; $n = 8$; Akt: WT control 100 ± 7%, WT DHPG 106 ± 6%, KO control 95 ± 6%, KO

DHPG 99 ± 9%; ANOVA treatment $p = 0.55$, genotype × treatment $p = 0.89$; $n = 8$; Figure 2D). Interestingly, a slight but significant decrease in ERK1/2 phosphorylation was seen in *Fmr1* KO CA1 suggesting the possibility of compensatory downregulation in response to elevated protein synthesis (t-test *$p < 0.008$; $n = 8$; Figure 2D). These results support the conclusion that ERK1/2 activation is neither elevated nor saturated in *Fmr1* KO hippocampus. Consistent with our previous results, no significant mGluR-mediated activation of Akt was observed in either WT or *Fmr1* KO CA1 (Figure 2D).

To test whether differences in mGluR-mediated signaling could be seen specifically at the synaptic level, we measured activation of ERK1/2 and Akt in synaptoneurosome fractions isolated from slices stimulated ± 100 μM DHPG for 5 minutes. Consistent with results from whole slices, we find that mGluR-mediated activation of ERK1/2 is preserved in *Fmr1* KO synaptoneurosomes (WT control 100 ± 8%, WT DHPG 135 ± 8%, KO control 98 ± 10%, KO DHPG 139 ± 9%; ANOVA treatment $p < 0.0001$, genotype × treatment $p = 0.68$; $n = 10$ sets of slices from 7 animals; Figure 2E). No activation of Akt was observed in either WT or *Fmr1* KO synaptoneurosomes (WT control 100 ± 9%, WT DHPG 102 ± 10%, KO control 98 ± 13%, KO DHPG 93 ± 13%; ANOVA treatment $p = 0.79$, genotype × treatment $p = 0.60$; $n = 10$ sets of slices from 7 animals; Figure 2E).

Our data suggest that the PI3K-Akt pathway is not basally hyperactive under conditions in which we observe excessive protein synthesis. To ensure that our assay was sensitive to changes in Akt activation, we exposed slices to insulin, a potent activator of the PI3K pathway (Proud, 2007). Results from these experiments show that a 10 minute application of 1 μM insulin leads to a robust activation of Akt in both *Fmr1* KO and WT slices (WT control 100 ± 6%, WT insulin 191 ± 16%, KO control 113 ± 21%, KO insulin 205 ± 20%; ANOVA treatment $p < 0.0005$, genotype × treatment $p = 0.979$; $n = 8$; Figure 2F). These results suggest that the PI3K-Akt pathway is preserved, and not saturated, in *Fmr1* KO slices.

Taken together, the results from these experiments show that differences in basal or evoked activation of mGluR5-mediated signaling do not parallel—and are therefore unlikely to account for—the differences in basal and DHPG-evoked protein synthesis in *Fmr1* KO hippocampus.

Inhibition of ERK1/2, but not mTOR, corrects excessive protein synthesis in the *Fmr1* KO

Our results show that the excessive protein synthesis in *Fmr1* KO can be corrected by inhibition of mGluR5, and that activation of Gp1 mGluRs leads to robust activation of ERK1/2. We therefore hypothesized that inhibition of ERK1/2 could, like MPEP, correct the excessive protein synthesis in the *Fmr1* KO. This hypothesis was tested using the MEK1/2-ERK1/2 inhibitor U0126, which we found robustly decreased ERK1/2 activation in WT and *Fmr1* KO at 5 μM (WT control 100 ± 15%, WT U0126 15 ± 3%; KO control 86 ± 8%, KO U0126 12 ± 2%; ANOVA treatment $p < 0.0001$; $n = 4$; Figure 3B). Slices were pre-incubated ± 5 μM U0126 for 30 minutes, and protein synthesis measured ± 5 μM U0126 for an additional 30 minutes. Our results reveal that U0126 corrects protein synthesis in the *Fmr1* KO down to WT levels (WT control 100 ± 6%, KO control 115 ± 4%, WT U0126 94 ± 6%; KO U0126 91 ± 6%; ANOVA genotype × treatment $p < 0.03$; $n = 9$; Figure 3B). These results provide the first evidence that downregulation of the ERK1/2 pathway is effective in correcting a core *Fmr1* KO phenotype.

In light of a recent study proposing that the Akt/mTOR pathway contributes to the exaggerated mGluR-LTD in the *Fmr1* KO (Sharma et al., 2010), we examined whether application of the mTOR antagonist rapamycin could rescue the excess protein synthesis in the *Fmr1* KO. Hippocampal slices were incubated ± 20 nM rapamycin for 30 minutes, then

metabolically labeled ± 20 nM rapamycin for 30 minutes. This treatment failed to correct the excess protein synthesis seen in the *Fmr1* KO (WT control 100 ± 5%, KO control 115 ± 6%, WT rapamycin 103 ± 3%, KO rapamycin 125 ± 8%; ANOVA genotype $p < 0.002$, ANOVA genotype × treatment $p = 0.51$; $n = 13$; Figure 3C). Rapamycin was confirmed to produce robust inhibition of mTOR by monitoring the phosphorylation of p70S6K, a direct downstream target (WT control 100 ± 19%, WT rapamycin 24 ± 5%; KO control 94 ± 14%, KO rapamycin 15 ± 4%; ANOVA treatment $p < 0.0001$, ANOVA genotype × treatment $p = 0.90$; $n = 7$; Figure 3C). These data suggest that the Akt-mTOR pathway does not contribute directly to the excessive protein synthesis seen in the *Fmr1* KO and might influence LTD by actions other than regulation of protein synthesis.

TrkB-mediated protein synthesis is occluded in the *Fmr1* KO

Results from our protein synthesis and signaling pathway experiments suggest that ERK1/2 links mGluR5 to protein synthesis, and that protein synthesis in the *Fmr1* KO is hypersensitive to the activation of this pathway (Figure 3D). This model would account for both the selective reduction of protein synthesis in the *Fmr1* KO with MPEP and U0126, and the selective increase in protein synthesis in the WT with DHPG stimulation (Figure 3D). A prediction of this model is that synaptic protein synthesis in response to any activator of ERK1/2 will be saturated in the *Fmr1* KO hippocampus. To test this idea, we looked at protein synthesis downstream of the BDNF receptor, TrkB, in WT and *Fmr1* KO slices. Activation of TrkB has been shown to result in ERK1/2-dependent protein synthesis at the synapse, and this is thought to play a role in sustained LTP (Kang and Schuman, 1996; Schratt et al., 2004; Kanhema et al., 2006).

Our goal was to test TrkB-mediated translation in our hippocampal slices; however, the penetration of BDNF in brain slices has been shown to vary considerably depending on experimental conditions (Kang et al., 1996). In addition, BDNF is known to activate p75-NTR, a receptor involved in cytotoxicity (Chao, 1994). Given these limitations, we chose to employ an antibody-based TrkB activation strategy. Dimerization of Trk receptors in response to agonist binding leads to autophosphorylation and initiation of downstream signaling cascades (Jing et al., 1992). Trk antibodies lead to the same activation, and have been shown to initiate the downstream signaling and functional consequences to the same degree as agonist application for both TrkA and TrkB (Clary et al., 1994; Qian et al., 2006).

To confirm that our monoclonal antibody activated TrkB, we applied 1 μg/ml to mature cultured hippocampal neurons for 15 minutes. Western blotting for p-Trk Tyr490 reveals that this treatment robustly activates TrkB, and occludes further activation via BDNF (control 100 ± 20%, control + BDNF 553 ± 53%, TrkB 849 ± 79%, TrkB + BDNF 897 ± 14%; ANOVA, BDNF $p < 0.002$, TrkB $p < 0.0001$, BDNF × TrkB, $p < 0.005$; $n = 4$ sets of cultures; Figure S3). Importantly, this treatment also results in strong ERK1/2 activation that mimics and occludes activation via BDNF (control 100 ± 3%, control + BDNF 173 ± 12%, TrkB 252 ± 20%, TrkB + BDNF 221 ± 22 %; ANOVA BDNF $p = 0.187$, TrkB $p < 0.002$, BDNF × TrkB $p < 0.02$; $n = 4$ sets of cultures; Figure S3). We therefore used this approach to measure TrkB-mediated translation in hippocampal slices. Slices were pre-incubated ± 1 μg/ml anti-TrkB for 30 minutes, then ActD ± 1 μg/ml anti-TrkB for another 30 minutes, and protein synthesis measured ± 1 μg/ml anti-TrkB for 1 hour (Kelleher et al., 2004). This treatment led to a significant increase in protein synthesis in WT slices, but failed to raise protein synthesis over the elevated basal level in *Fmr1* KO slices (WT control 100 ± 6%, WT TrkB 132 ± 6%, KO control 121 ± 6%, KO TrkB 113 ± 9%; ANOVA genotype × treatment $p < 0.02$; $n = 6$; Figure 4). These results suggest that, similar to mGluR-mediated protein synthesis, TrkB-mediated protein synthesis is occluded (and therefore dysregulated) in the *Fmr1* KO hippocampus. This finding is interesting in light of a recent study showing that BDNF-TrkB facilitated LTP is deficient in the *Fmr1* KO (Lauterborn et al., 2007). It is

possible that the inability of TrkB to elicit further protein synthesis in the *Fmr1* KO is related to this phenotype.

Inhibition of ERK1/2 eliminates audiogenic seizures in the *Fmr1* KO

If hypersensitivity to ERK1/2 pathway signaling is a core cause of pathological changes in the *Fmr1* KO, then treatment with an inhibitor of the ERK1/2 pathway might be expected to correct other phenotypes in the *Fmr1* KO. Enhanced susceptibility to audiogenic seizures (AGS) is one of the most robust phenotypes observed in the *Fmr1* KO mouse, and models the epilepsy seen in FXS patients (Berry-Kravis, 2002; Yan et al., 2005). Acute injection of MPEP has been shown to ameliorate the AGS phenotype in *Fmr1* KO mice (Yan et al., 2005), and we wanted to test whether acute injection a brain-penetrant MEK1/2-ERK1/2 inhibitor (SL 327), could do the same. *Fmr1* KO and WT mice were injected i.p. with 100 mg/kg SL 327 (based on Zhong et al., 2009) or 50% DMSO vehicle, and returned to their home cage for one hour. To initiate AGS, mice were transferred to a plastic test cage and exposed to a seizure-inducing alarm for 2 minutes. During stimulus presentation, mice were scored for four stages of AGS: wild running, clonic seizure, tonic seizure, and death (Yan et al., 2005; Dolen et al., 2007; Zhong et al., 2009). All animals were injected and scored blind to genotype.

Consistent with previous studies, we observed that vehicle-treated *Fmr1* KO mice exhibited a 73% incidence of AGS, in stark contrast to the 0% incidence observed in vehicle-treated WT mice (Fisher's exact test *$p < 0.03$; Table 3) (Yan et al., 2005; Dolen et al., 2007). Strikingly, SL 327 treatment completely eliminated AGS in the *Fmr1* KO, dropping the incidence to 0% (Fisher's exact test *$p < 0.03$; Table 3). These results provide the first evidence that inhibition of ERK1/2 can correct *in vivo* phenotypes observed in the *Fmr1* KO.

We also tested the hypothesis that rapamycin can inhibit AGS, based on recent evidence that mTOR signaling is altered in some biochemical preparations of *Fmr1* KO brain (Sharma et al., 2010). *Fmr1* KO and WT mice were injected i.p. with 6 mg/kg rapamycin (based on Ehninger et al., 2008 and Meikle et al., 2008) or 100% DMSO vehicle, and tested for AGS after 1 hour. Unlike the ERK inhibitor, rapamycin failed to significantly reduce the incidence of AGS in the *Fmr1* KO (Fisher's exact test KO vehicle vs. WT vehicle *$p < 0.005$, KO vehicle vs. KO rapamycin $p = 0.372$; Table 4). Together, these results suggest that acute inhibition of ERK1/2, but not mTOR, can correct the AGS phenotype in the *Fmr1* KO.

Discussion

Although reduction of mGluR5 activity has been shown to correct multiple phenotypes in the *Fmr1* KO mouse (Aschrafi et al., 2005; Yan et al., 2005; Tucker et al., 2006; Dolen et al., 2007; Nakamoto et al., 2007; de Vrij et al., 2008; Qiu et al., 2008), the molecular basis has been unclear. We show here, for the first time, that acute pharmacological inhibition of either mGluR5 or the ERK1/2 signaling pathway is sufficient to normalize protein synthesis in *Fmr1* KO hippocampus to WT levels. The elevated protein synthesis observed in the *Fmr1* KO mimics and occludes any further increases with DHPG stimulation. However, neither basal nor stimulated activation of either the MAPK or PI3K signaling pathways were found to be increased in the *Fmr1* KO. Thus, the cause of increased protein synthesis in the *Fmr1* KO brain appears to be increased sensitivity of the protein synthetic machinery to mGluR5-ERK1/2 signaling, rather than increased mGluR5-ERK1/2 signaling *per se* (Figure 5). Consistent with this model, we find that protein synthesis stimulated via another synaptic activator of ERK1/2, the TrkB receptor, is also saturated in *Fmr1* KO hippocampus. Hypersensitivity to ERK1/2 pathway activation appears to be relevant to the disorder *in vivo*

as we found that pharmacological antagonism of this pathway completely eliminates the AGS phenotype in the *Fmr1* KO.

A well-documented mechanism of translational control is the modulation of mRNA availability to the ribosome (Richter, 2007). Given that FMRP has been estimated to bind 4% of all brain mRNAs (Ashley et al., 1993), it is possible that de-repression and "leaky" translation of these mRNAs in response to basal ERK1/2 signaling causes the elevated protein synthesis seen in the *Fmr1* KO. Consistent with this idea, the mRNA granule population, thought to represent translationally dormant mRNAs, is reduced in the brains of *Fmr1* KO versus WT mice (Aschrafi et al., 2005). Furthermore, acute *in vivo* administration of MPEP in the *Fmr1* KO animals was sufficient to shift the mRNA granule population closer to the WT value. Considered together with the current findings, the data suggest that mGluR5 is a major initiator of activity-regulated synaptic protein synthesis in the brain, and that constitutive mGluR5-ERK1/2 signaling is responsible for much of the excessive protein synthesis in the *Fmr1* KO under basal conditions.

Basal protein synthesis in the WT hippocampal slice preparation was not significantly reduced by either U0126 or rapamycin (Figure 3), but was eliminated by cycloheximide (Figure S1). Although it is possible that increased exposure to the inhibitors might reveal some inhibition of protein synthesis (e.g., Kelleher et al., 2004; Nie et al., 2010), the treatments we used were sufficient to produce substantial inhibition of MEK and mTOR enzymatic activity as assayed by reduced levels of phosphorylated ERK and p70S6K, respectively. Thus, the data suggest that under the conditions of our experiments, basal ERK and mTOR signaling contribute little to basal protein synthesis in the WT. The residual protein synthesis in the presence of inhibitors is either constitutive or driven by other signaling pathways.

Activation of mGluRs has been shown to stimulate the ERK1/2 pathway in a wide variety of systems, including cell lines (Ferraguti et al., 1999), cultured neurons (Mao et al., 2005), striatum (Choe and Wang, 2001), spinal cord (Adwanikar et al., 2004), hippocampal slice (Berkeley and Levey, 2003; Gallagher et al., 2004), and retinal pigment epithelial cells (Garcia et al., 2008). Although recent studies have shown an activation of Akt (Hou and Klann, 2004; Sharma et al., 2010) and mTOR (Antion et al., 2008; Ronesi and Huber, 2008; Sharma et al., 2010) in response to Gp1 mGluR activation, we did not observe this under the conditions of our experiment. It is possible that this pathway is activated by DHPG at earlier or later time points following stimulation than what we examined. However, the data do indicate that this pathway is not hyperactive under basal conditions in *Fmr1* KO slices that exhibit excessive protein synthesis. Failure to observe increased activation of either ERK1/2 or Akt pathways under basal conditions is not accounted for by an insensitivity of our assay to detect increases, as evidenced by the effects of DHPG on ERK and insulin on Akt (Figure 2).

Our findings contrast with a recent study by Sharma *et al.* (2010) who showed increased Akt-mTOR pathway activation in the *Fmr1* KO hippocampus, attributed by the authors to be caused by elevated expression of the PI3K enhancer protein PIKE (Sharma et al., 2010). One key difference between our study and theirs is the preparation of the *Fmr1* KO tissue. Our preparation was optimized to measure differences in protein metabolism in a physiologically stable tissue slice whereas theirs was optimized to capture early postmortem differences in protein phosphorylation. To ensure that we could replicate their findings, we probed the status of Akt and mTOR phosphorylation in homogenates from rapidly dissected hippocampus and similarly observed an increase in p-Akt and p-mTOR in *Fmr1* KO relative to WT (Figure S4). This difference observed in freshly dissected tissue could reflect the status *in vivo* or, equally likely, a differential response to postmortem stress such as anoxia

or rapid cooling. Regardless, our results strongly suggest that elevated Akt-mTOR signaling is not a cause of elevated protein synthesis in the *Fmr1* KO (Figure 5). Firstly, we do not see evidence for increased Akt-mTOR signaling under experimental conditions that reveal an elevation in hippocampal protein synthesis quantitatively identical to the status *in vivo* (Qin et al., 2005). Secondly, the mTOR inhibitor rapamycin does not affect the basal increase in protein synthesis in the *Fmr1* KO slices. As Sharma *et al*. suggest, increased activation of the Akt-mTOR pathway could be a consequence of overexpression of the regulatory protein PIKE. In this case, it seems more appropriate to view differences in the mTOR pathway as a consequence rather than a cause of increased mGluR5-regulated protein synthesis in the *Fmr1* KO. That aberrant mTOR pathway activation may be distal to increased protein synthesis in fragile X in no way diminishes the possible therapeutic significance of that discovery. However, our finding that rapamycin treatment fails to prevent AGS (Table 4) suggests that elevated mTOR activity may not be centrally involved in epileptogenesis associated with FXS.

Our results showing that protein synthesis downstream of TrkB activation is saturated in the *Fmr1* KO, and that inhibition of ERK1/2 signaling can correct excessive protein synthesis, suggest that a core defect in FXS is leaky translation in response to ERK1/2 activity. Supporting this, we show that acute pharmacological antagonism of ERK1/2 completely rescues the AGS phenotype in the *Fmr1* mouse (Table 3). Although the major regulator of the relevant protein synthesis activity at excitatory synapses is mGluR5, it seems likely that other neurotransmitter systems that signal via ERK1/2 can contribute to the pathophysiology of FXS. This insight suggests the possibility of additional therapeutic targets besides mGluR5 for the treatment of the core pathophysiology of this disorder in humans.

Supplementary Material

Refer to Web version on PubMed Central for supplementary material.

Acknowledgments

For excellent technical support and helpful discussions we wish to thank the following: Kathleen “Barbara” Oram, Suzanne Meagher, Erik Sklar, Arnold Heynen, Genevieve Conley, Cornelia Hall, Eugenia Gisin, Stephanie Lacy, Charlotte Yang, Lena Khibnik, Monica Linden, Rahmat Muhammad, Bridget Dolan, Gül Dölen, and Gordon Smith. This work was supported in part by grants from FRAXA, NIMH, NICHD, Simons Foundation and the Hillibrand Foundation.

References

Adwanikar H, Karim F, Gereau RWt. Inflammation persistently enhances nocifensive behaviors mediated by spinal group I mGluRs through sustained ERK activation. Pain. 2004; 111:125–135. [PubMed: 15327816]

Ashley CT Jr, Wilkinson KD, Reines D, Warren ST. FMR1 protein: conserved RNP family domains and selective RNA binding. Science. 1993; 262:563–566. [PubMed: 7692601]

Avruch J, Belham C, Weng Q, Hara K, Yonezawa K. The p70 S6 kinase integrates nutrient and growth signals to control translational capacity. Prog Mol Subcell Biol. 2001; 26:115–154. [PubMed: 11575164]

Bear MF, Huber KM, Warren ST. The mGluR theory of fragile X mental retardation. Trends Neurosci. 2004; 27:370–377. [PubMed: 15219735]

Chao MV. The p75 neurotrophin receptor. J Neurobiol. 1994; 25:1373–1385. [PubMed: 7852992]

Dolen G, Bear MF. Role for metabotropic glutamate receptor 5 (mGluR5) in the pathogenesis of fragile X syndrome. J Physiol. 2008; 586:1503–1508. [PubMed: 18202092]

Ehninger D, Han S, Shilyansky C, Zhou Y, Li W, Kwiatkowski DJ, Ramesh V, Silva AJ. Reversal of learning deficits in a Tsc2+/− mouse model of tuberous sclerosis. Nat Med. 2008; 14:843–848. [PubMed: 18568033]

Gallagher SM, Daly CA, Bear MF, Huber KM. Extracellular signal-regulated protein kinase activation is required for metabotropic glutamate receptor-dependent long-term depression in hippocampal area CA1. J Neurosci. 2004; 24:4859–4864. [PubMed: 15152046]

Garcia S, Lopez E, Lopez-Colome AM. Glutamate accelerates RPE cell proliferation through ERK1/2 activation via distinct receptor-specific mechanisms. J Cell Biochem. 2008; 104:377–390. [PubMed: 18022816]

Gingras AC, Raught B, Sonenberg N. eIF4 initiation factors: effectors of mRNA recruitment to ribosomes and regulators of translation. Annu Rev Biochem. 1999; 68:913–963. [PubMed: 10872469]

Hara K, Yonezawa K, Weng QP, Kozlowski MT, Belham C, Avruch J. Amino acid sufficiency and mTOR regulate p70 S6 kinase and eIF-4E BP1 through a common effector mechanism. J Biol Chem. 1998; 273:14484–14494. [PubMed: 9603962]

Huber KM, Gallagher SM, Warren ST, Bear MF. Altered synaptic plasticity in a mouse model of fragile X mental retardation. Proc Natl Acad Sci U S A. 2002; 99:7746–7750. [PubMed: 12032354]

Jing S, Tapley P, Barbacid M. Nerve growth factor mediates signal transduction through trk homodimer receptors. Neuron. 1992; 9:1067–1079. [PubMed: 1281417]

Kang H, Jia LZ, Suh KY, Tang L, Schuman EM. Determinants of BDNF-induced hippocampal synaptic plasticity: role of the Trk B receptor and the kinetics of neurotrophin delivery. Learn Mem. 1996; 3:188–196. [PubMed: 10456089]

Kelleher RJ 3rd, Govindarajan A, Jung HY, Kang H, Tonegawa S. Translational control by MAPK signaling in long-term synaptic plasticity and memory. Cell. 2004; 116:467–479. [PubMed: 15016380]

Kirov SA, Sorra KE, Harris KM. Slices have more synapses than perfusion-fixed hippocampus from both young and mature rats. J Neurosci. 1999; 19:2876–2886. [PubMed: 10191305]

Lauterborn JC, Rex CS, Kramar E, Chen LY, Pandyarajan V, Lynch G, Gall CM. Brain-derived neurotrophic factor rescues synaptic plasticity in a mouse model of fragile X syndrome. J Neurosci. 2007; 27:10685–10694. [PubMed: 17913902]

Lipton P, Raley-Susman KM. Autoradiographic measurements of protein synthesis in hippocampal slices from rats and guinea pigs. Methods. 1999; 18:127–143. [PubMed: 10356343]

Mao L, Yang L, Tang Q, Samdani S, Zhang G, Wang JQ. The scaffold protein Homer1b/c links metabotropic glutamate receptor 5 to extracellular signal-regulated protein kinase cascades in neurons. J Neurosci. 2005; 25:2741–2752. [PubMed: 15758184]

Meikle L, Pollizzi K, Egnor A, Kramvis I, Lane H, Sahin M, Kwiatkowski DJ. Response of a neuronal model of tuberous sclerosis to mammalian target of rapamycin (mTOR) inhibitors: effects on mTORC1 and Akt signaling lead to improved survival and function. J Neurosci. 2008; 28:5422–5432. [PubMed: 18495876]

Nie D, Di Nardo A, Han JM, Baharanyi H, Kramvis I, Huynh T, Dabora S, Codeluppi S, Pandolfi PP, Pasquale EB, Sahin M. Tsc2-Rheb signaling regulates EphA-mediated axon guidance. Nat Neurosci. 2010; 13:163–172. [PubMed: 20062052]

Proud CG. Signalling to translation: how signal transduction pathways control the protein synthetic machinery. Biochem J. 2007; 403:217–234. [PubMed: 17376031]

Qin M, Kang J, Burlin TV, Jiang C, Smith CB. Postadolescent changes in regional cerebral protein synthesis: an in vivo study in the FMR1 null mouse. J Neurosci. 2005; 25:5087–5095. [PubMed: 15901791]

Richter JD. CPEB: a life in translation. Trends Biochem Sci. 2007; 32:279–285. [PubMed: 17481902]

Sajikumar S, Navakkode S, Frey JU. Protein synthesis-dependent long-term functional plasticity: methods and techniques. Curr Opin Neurobiol. 2005; 15:607–613. [PubMed: 16150586]

Sharma A, Hoeffer CA, Takayasu Y, Miyawaki T, McBride SM, Klann E, Zukin RS. Dysregulation of mTOR signaling in fragile X syndrome. J Neurosci. 2010; 30:694–702. [PubMed: 20071534]

Shaul YD, Seger R. The MEK/ERK cascade: from signaling specificity to diverse functions. Biochim Biophys Acta. 2007; 1773:1213–1226. [PubMed: 17112607]

Wang X, Beugnet A, Murakami M, Yamanaka S, Proud CG. Distinct signaling events downstream of mTOR cooperate to mediate the effects of amino acids and insulin on initiation factor 4E-binding proteins. Mol Cell Biol. 2005; 25:2558–2572. [PubMed: 15767663]

Whittingham TS, Lust WD, Christakis DA, Passonneau JV. Metabolic stability of hippocampal slice preparations during prolonged incubation. J Neurochem. 1984; 43:689–696. [PubMed: 6086837]

Yan QJ, Rammal M, Tranfaglia M, Bauchwitz RP. Suppression of two major Fragile X Syndrome mouse model phenotypes by the mGluR5 antagonist MPEP. Neuropharmacology. 2005; 49:1053–1066. [PubMed: 16054174]

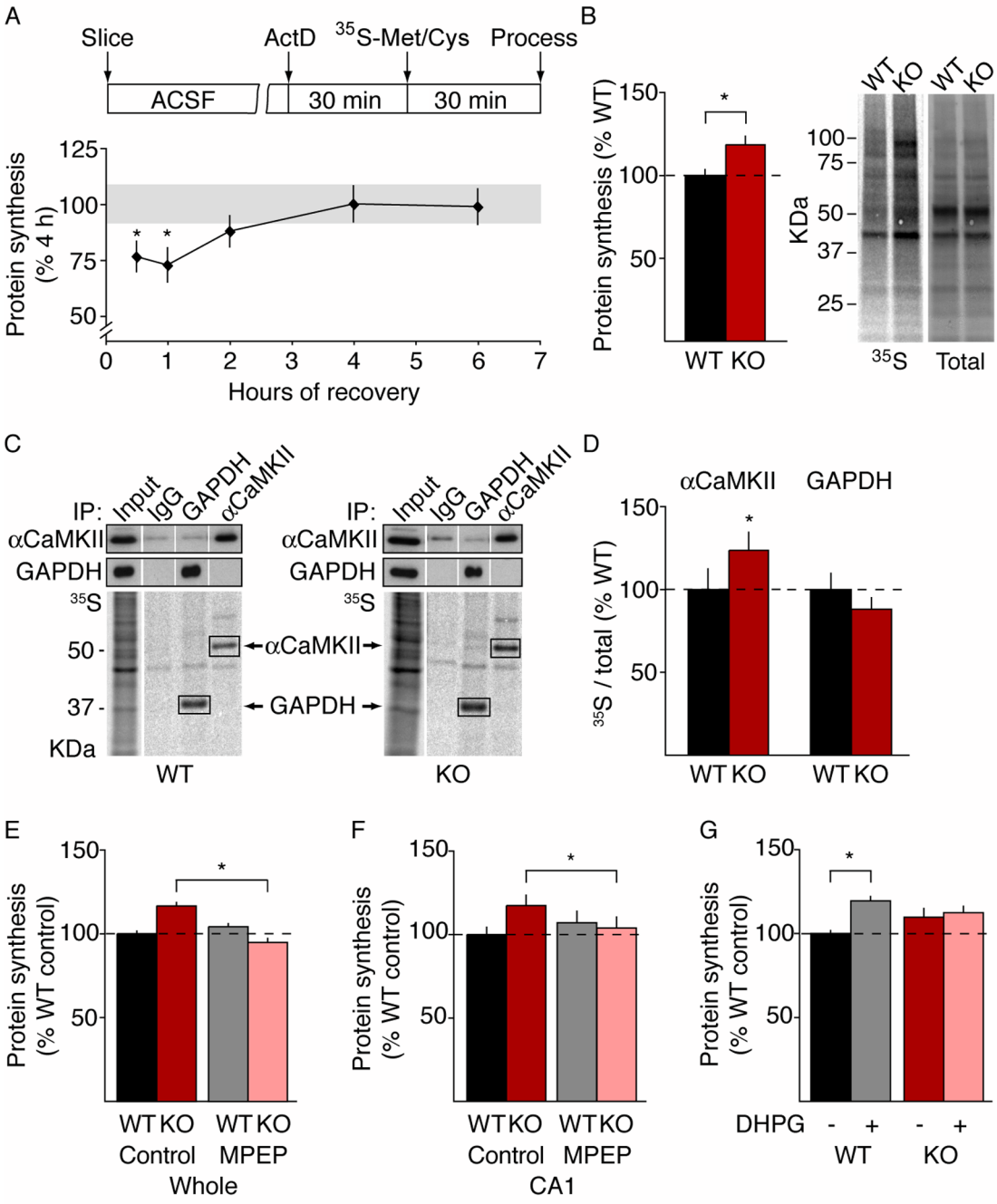

Figure 1. Exaggerated protein synthesis in *Fmr1* KO is ameliorated by mGluR5 antagonism and mimicked by mGluR activation in WT

(A) Schematic illustrates experimental timeline: hippocampal slices were recovered in ACSF, incubated with 25 μM ActD for 30 min, then protein synthesis was measured with 10 μCi/ml ^{35}S-Met/Cys for 30 min. To measure the effect of post-slice recovery time on protein synthesis, slices were incubated in ACSF for 0 h, 0.5 h, 1.5 h, 3.5 h, or 5.5 h before exposure to ActD and metabolic labeling. Quantification of multiple experiments showed that a 4 h post-slice recovery time yields maximal protein synthesis, which is stable for at least another 2 h (ANOVA $p < 0.05$; t-test: 4 h vs. 0.5 h *$p < 0.04$, 4 h vs. 1 h *$p < 0.03$, 4 h vs. 6 h $p = 0.89$; $n = 10$). ***(B)*** Protein synthesis was elevated in *Fmr1* KO versus WT hippocampus (t-

test *p < 0.02; n = 13). Differences in protein synthesis are exemplified by representative autoradiographs and total protein stain of the same membrane. ***(C)*** Representative immunoblots and autoradiographs show IPs for alpha-CaMKII and GAPDH from WT and *Fmr1* KO slices metabolically labeled with 50 μCi/ml ^{35}S-Met/Cys for 1 hour. ***(D)*** Quantification of multiple experiments reveals that the ratio of ^{35}S-incorporated total alpha-CaMKII is higher in *Fmr1* KO slices than WT slices (t-test *p < 0.04; n = 6). In contrast, the ratio of ^{35}S-incorporated : total GAPDH is not elevated in *Fmr1* KO versus WT slices (t-test p = 0.31; n = 5). ***(E)*** During the first 5 minutes of metabolic labeling, WT and *Fmr1* KO slices were exposed to 50 μM MPEP or vehicle. Quantification of multiple experiments shows that MPEP treatment corrects protein synthesis in *Fmr1* KO back to WT levels (t-test *p < 0.03; n = 8). This treatment had no significant effect on WT protein synthesis (t-test p = 0.58; n = 8). ***(F)*** WT and *Fmr1* KO slices were pre-incubated ± 10 μM MPEP for 30 min, then metabolically labeled ± 10 μM MPEP for 30 min. Measurements taken from isolated CA1 regions show that MPEP corrects excessive protein synthesis in *Fmr1* KO CA1 back to WT levels (t-test *p < 0.02; n = 8). This treatment had no effect on WT CA1 (t-test p = 0.24; n = 8). ***(G)*** WT and *Fmr1* KO slices were stimulated ± 100 μM DHPG during the first 5 minutes of metabolic labeling. DHPG stimulation caused a robust increase in protein synthesis in WT (t-test *p < 0.0001), but not *Fmr1* KO (t-test p = 0.62), hippocampus (n = 8). N represents number of animals per group, where 1–2 slices were analyzed per animal. Error bars represent SEM.

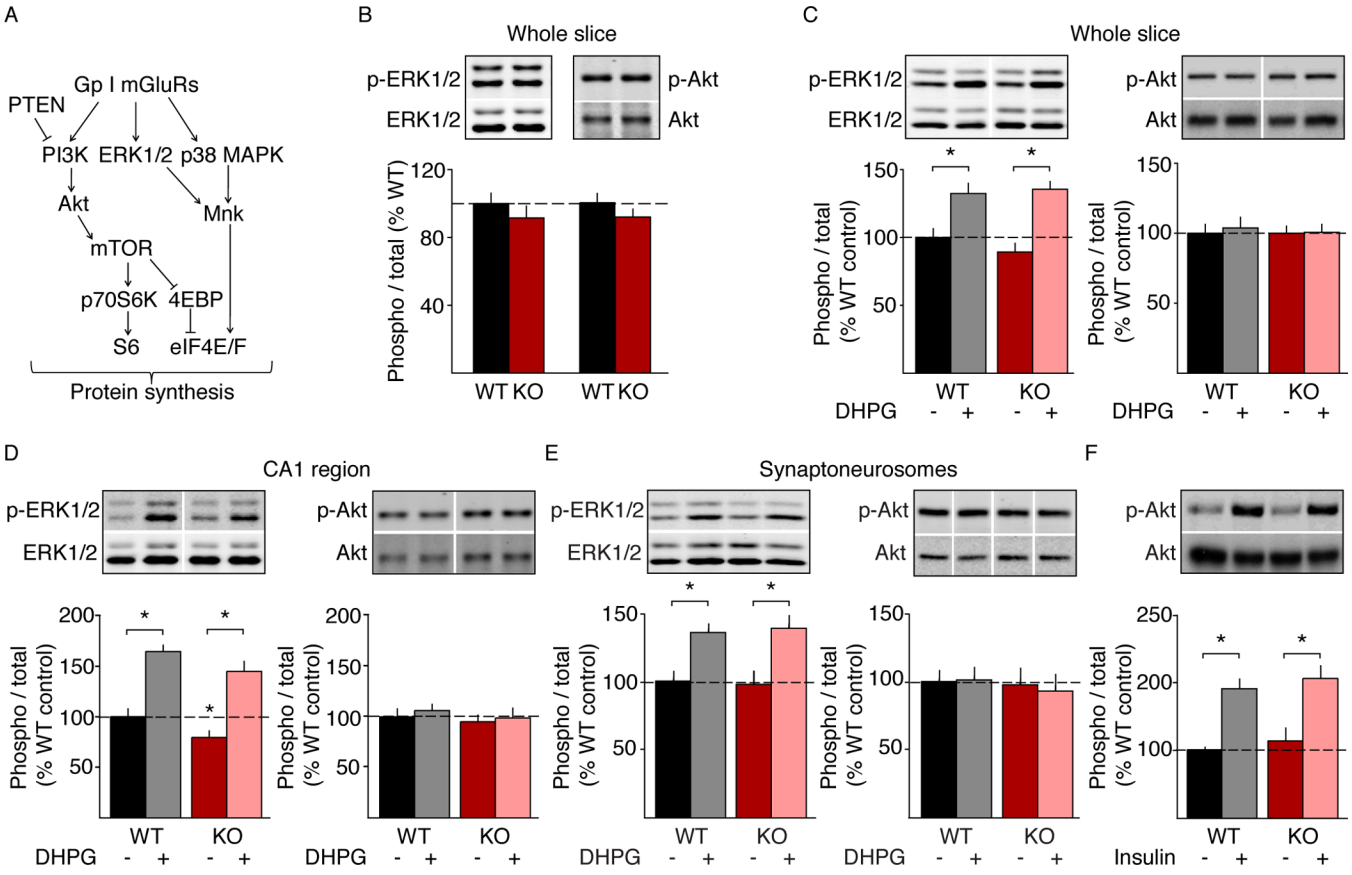

Figure 2. Basal and DHPG-evoked MAPK and PI3K signaling appear normal in the *Fmr1* KO

(A) Schematic shows signaling components of the PI3K and MAPK families thought to be downstream of mGluR5 (Proud, 2007). ***(B)*** Basal activation (phosphorylation) states of ERK1/2 and Akt were measured in untreated hippocampal slices from WT and *Fmr1* KO, the majority of which were used for the assay of basal protein synthesis. Results reveal no difference in either ERK1/2 (t-test p = 0.223) or Akt (t-test p = 0.12) activation in *Fmr1* KO versus WT (n = 27). ***(C)*** Gp1 mGluR-mediated activation of ERK1/2 was measured immediately after application of 100 μM DHPG for 5 min. Results reveal that DHPG significantly increases ERK1/2 activation in both WT (t-test *p < 0.0001) and *Fmr1* KO (t-test *p < 0.0001) slices (n = 14). Interestingly, activation of Akt was not observed in either WT (t-test p = 0.47) or *Fmr1* KO (t-test p = 0.96) slices (n = 14). ***(D)*** ERK1/2 and Akt activation was measured in microdissected CA1 after 5 min application of 100 μM DHPG. Analyses reveal that stimulation of Gp1 mGluRs leads to a significant activation of ERK1/2 in both WT (t-test *p < 0.0001) and *Fmr1* KO (t-test *p < 0.006) CA1 (n = 8). A slight but significant reduction in basal ERK1/2 activation is seen in *Fmr1* KO CA1 (t-test *p < 0.008). Basal activation of Akt in *Fmr1* KO CA1 is not significantly different from WT CA1 (t-test p = 0.65), and no activation of Akt is observed in either WT (t-test p = 0.61) or *Fmr1* KO (t-test p = 0.76) CA1 (n = 8). ***(E)*** Synaptoneurosomes were isolated from sets of slices treated with 100 μM DHPG for 5 min, and levels of ERK1/2 and Akt activation were assessed. Results reveal a significant activation of ERK1/2 in both WT (t-test *p < 0.001) and *Fmr1* KO (t-test *p < 0.01) synaptoneurosomes (n = 10 sets of slices from 7 animals). No activation of Akt was observed in either WT (t-test p = 0.88) or *Fmr1* KO (t-test p = 0.47) synaptoneurosomes (n = 10 sets of slices from 7 animals). ***(F)*** Activation of Akt was measured after a 10 min application of 1 μM insulin. Results reveal a robust activation of Akt in both WT (t-test *p < 0.001) and *Fmr1* KO (t-test *p < 0.05) slices (n = 8).

Representative immunoblots reflect quantified results. Unless otherwise noted, n represents number of animals per group, where 1–2 slices were analyzed per animal. Error bars represent SEM.

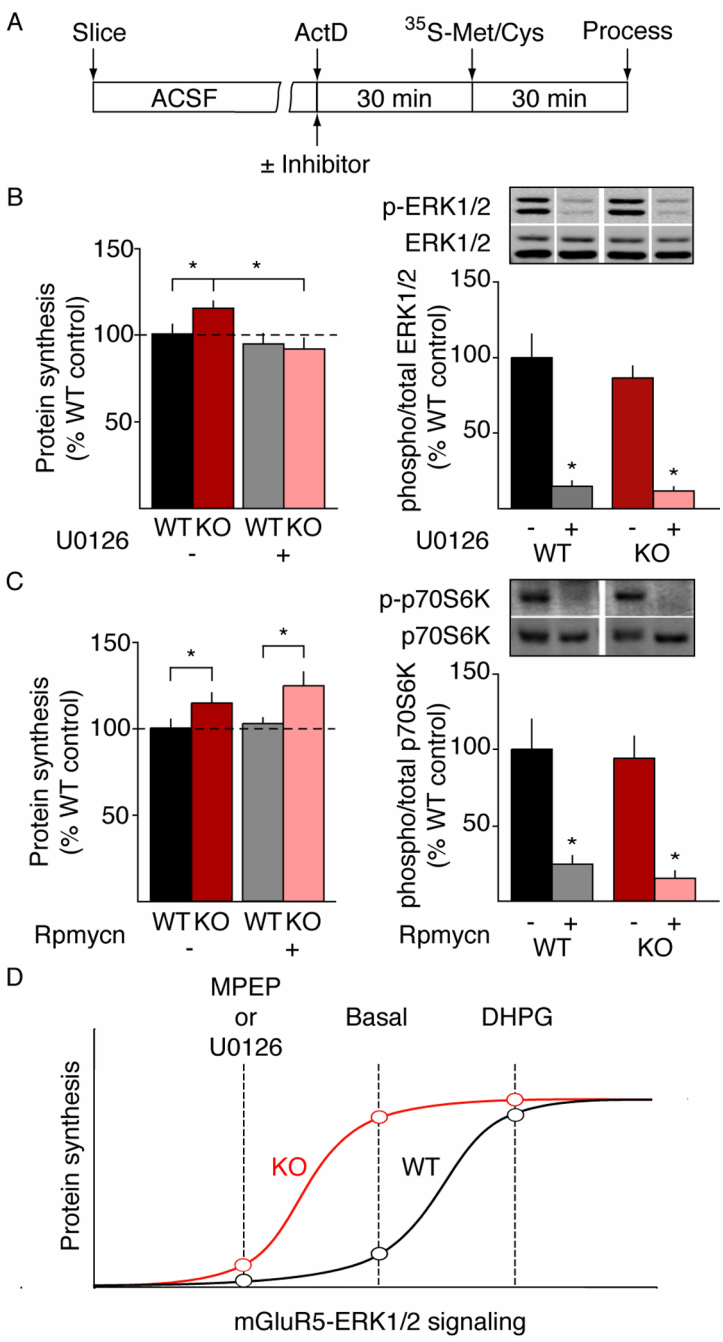

Figure 3. Inhibition of ERK1/2, but not mTOR, corrects excessive protein synthesis in the *Fmr1* KO

(A) Schematic illustrates experimental timeline: WT and *Fmr1* KO hippocampal slices are recovered, incubated with 25 μM ActD ± inhibitor for 30 min, then protein synthesis measured ± inhibitor for 30 min. ***(B)*** Protein synthesis and ERK1/2 activation were measured in slices incubated ± 5 μM U0126. Exposure to 5 μM U0126 significantly reduces protein synthesis in *Fmr1* KO (t-test *p < 0.006), but not WT (t-test p = 0.15) slices (n = 9). This concentration of U0126 significantly reduced ERK1/2 activation in both WT (t-test *p < 0.01) and *Fmr1* KO (t-test *p < 0.005) slices (n = 4). ***(C)*** Protein synthesis and p70S6K activation were measured in slices incubated ± 20 nM rapamycin. Exposure to 20 nM

rapamycin does not correct protein synthesis in the *Fmr1* KO (WT control vs. KO control t-test *p < 0.03; WT rapamycin vs. KO rapamycin t-test *p < 0.02; n = 13). This dose of rapamycin robustly reduces p70S6K activation in both WT (t-test *p < 0.02) and *Fmr1* KO (t-test *p < 0.002) slices (n = 7). Quantified changes are shown in representative immunoblots. N represents number of animals per group, where 1–2 slices were analyzed per animal. Error bars represent SEM. ***(D)*** Our results suggest the illustrated model of the relationship between mGluR5-mediated ERK1/2 activation and synaptic protein synthesis in WT and *Fmr1* KO. In *Fmr1* KO, the loss of FMRP renders the activation of protein synthesis the more sensitive to basal levels of mGluR5-ERK1/2 activity. Inhibition of basal mGluR5-ERK1/2 with MPEP or U0126 leads to a significant decrease in *Fmr1* KO, but not WT protein synthesis due to this hypersensitivity. Conversely, DHPG does not elevate of protein synthesis in *Fmr1* KO because mGluR5-ERK1/2-mediated protein synthesis is already saturated.

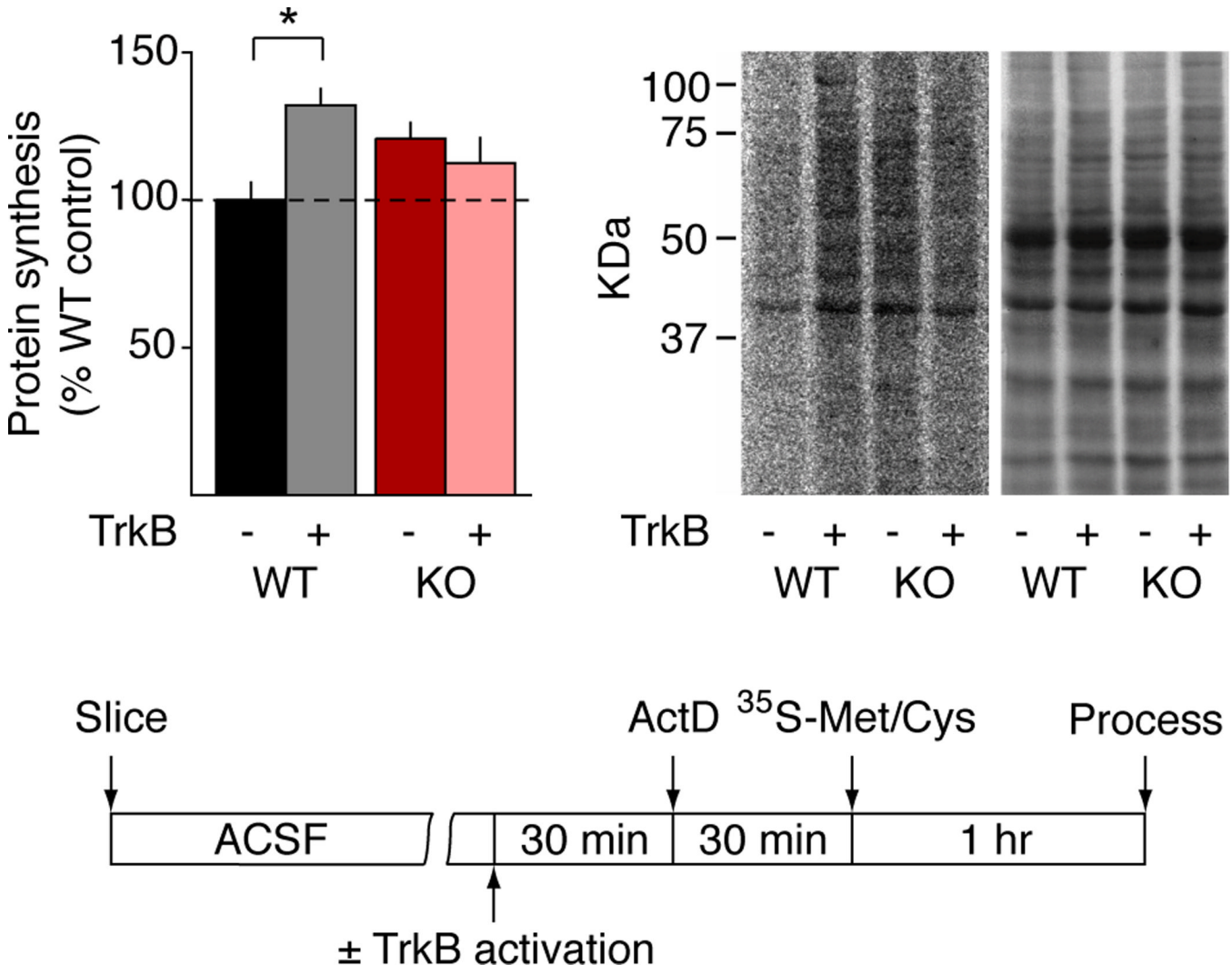

Figure 4. TrkB-mediated protein synthesis is mimicked and occluded in the *Fmr1* KO

WT and *Fmr1* KO hippocampal slices were recovered, pre-incubated ±1 μg/ml anti-TrkB for 30 min, then 25 μM ActD ±1 μg/ml anti-TrkB for an additional 30 min, and 1 h of protein synthesis measured ±1 μg/ml anti-TrkB. Results show that TrkB activation leads to a significant increase in protein synthesis in WT (t-test *$p < 0.03$) but not *Fmr1* KO (t-test $p = 0.433$) slices ($n = 6$). Schematic illustrates the time course of the experiment. Quantified differences are exemplified by representative autoradiograph and total protein stain of the same membrane. N represents number of animals per group, where 1–2 slices were analyzed per animal. Error bars represent SEM.

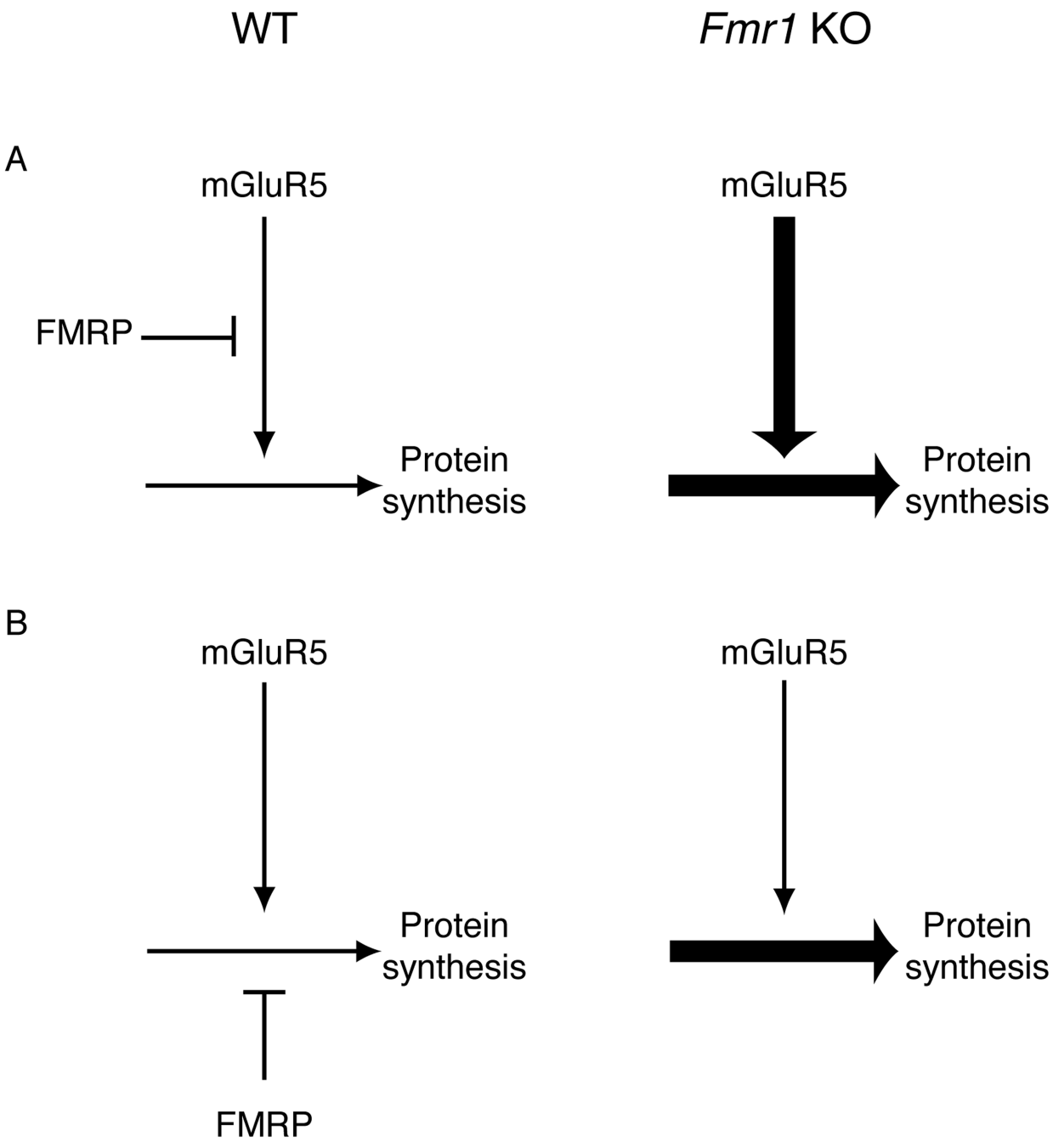

Figure 5. Heuristic models of the interaction between mGluR5 and FMRP

Illustrated are simple logical relationships between FMRP and mGluR5-stimulated synaptic protein synthesis. ***(A)*** The finding of elevated protein synthesis downstream of constitutive mGluR5 activation suggested a model in which FMRP or an FMRP-regulated protein specifically inhibits the signaling pathway that couples mGluR5 to translation initiation (Hou et al., 2006; Sharma et al., 2010). (***B***) An alternative to the model in which signaling is unaffected in the absence of FMRP, but the consequences on protein synthesis are exaggerated. The results of the current investigation favor model ***B***.

Table 1

No basal upregulation of MAPK or PI3K pathways in the *Fmr1* KO

Basal activation (phosphorylation) states of ERK1/2, p38, and the PI3K pathway proteins PTEN, Akt, mTOR, p70S6K and S6 were measured untreated hippocampal slices from *Fmr1* KO and WT, the majority of which were used for measurement of protein synthesis. Results are expressed as % average WT ± SEM. For all proteins, no significant increase was seen in *Fmr1* KO as compared to WT. In contrast, a small but significant decrease in the activation state of p38 (t-test *p < 0.05) was observed in *Fmr1* KO. For each animal, 1–2 slices were analyzed. ERK1/2 and Akt data are graphically represented in Figure 2.

Protein	Phosphorylation site	Phospho / total		Animals
		WT	KO	
Erk1/2	Thr202/Tyr204	100 ± 6 %	92 ± 7 %	27
Akt	Ser473	100 ± 6 %	92 ± 4 %	27
p38 *	Thr180/Tyr182	100 ± 8 %	85 ± 7 %	10
PTEN	Ser380/Thr382/383	100 ± 13 %	100 ± 11 %	10
mTOR	Ser2448	100 ± 7 %	111 ± 8 %	16
p70S6K	Thr389	100 ± 8 %	102 ± 6 %	19
S6	Ser235/236	100 ± 12 %	79 ± 7 %	17

T-test *p < 0.05

Table 2

No difference in mGluR-stimulated MAPK or PI3K activation in the *Fmr1* KO

Hippocampal slices were stimulated with 100 μM DHPG or vehicle for exactly 5 min. Activation states of ERK1/2, p38, and the PI3K pathway proteins PTEN, Akt, mTOR, p70S6K and S6 were measured in *Fmr1* KO and WT. Results are expressed as % average WT control ± SEM. Of the proteins examined, only ERK1/2 was activated by Gp 1 mGluR stimulation (ANOVA treatment $p < 0.0001$, genotype × treatment $p = 0.07$). This increase was seen in both WT (t-test *$p < 0.0001$) and *Fmr1* KO (t-test *$p < 0.0001$). A small but significant decrease in the activation state of p38 was also observed in *Fmr1* KO (t-test *$p < 0.05$). For each animal, 1–2 slices were analyzed. Data from untreated slices are incorporated in the data set shown in Table 1; ERK1/2 and Akt data are graphically represented in Figure 2.

Protein	Phosphorylation site	Phospho / total				Animals
		WT	WT + DHPG	KO	KO + DHPG	
Erk1/2 *	Thr202/Tyr204	100 ± 6 %	132 ± 8 %	90 ± 6 %	135 ± 6 %	13
Akt	Ser473	100 ± 5 %	104 ± 6 %	100 ± 5 %	100 ± 6 %	14
p38	Thr180/Tyr182	100 ± 5 %	112 ± 9 %	84 ± 5 %	94 ± 7 %	9
PTEN	Ser380/Thr382/383	100 ± 10 %	91 ± 11 %	80 ± 11 %	94 ± 12 %	7
mTOR	Ser2448	100 ± 11 %	105 ± 8 %	117 ± 12 %	102 ± 5 %	12
p70S6K	Thr389	100 ± 7 %	105 ± 3 %	119 ± 7 %	100 ± 9 %	8
S6	Ser235/236	100 ± 10 %	97 ± 9 %	85 ± 10 %	83 ± 3 %	6

ANOVA treatment *$p < 0.0001$

Table 3

Acute ERK1/2 inhibition eliminates AGS in the *Fmr1* KO

Young (P18–22) *Fmr1* KO and WT mice were injected with 100 mg/kg SL 327 or vehicle (50% DMSO). After 1 hour mice were exposed to a seizure-inducing stimulus for 2 minutes, and scored for four stages of AGS: wild running (WR; pronounced, undirected running and thrashing), clonic seizure (violent spasms accompanied by loss of balance), tonic seizure (postural rigidity in limbs), and death. Results reveal that treatment with SL 327 eliminates AGS in *Fmr1* KO mice (Fisher's exact test: KO control vs. WT control *p < 0.03, KO control vs. KO SL 327 *p < 0.02, KO control vs. WT SL 327 *p < 0.03).

	Incidence	Wild running	Clonic	Tonic	Death
KO Vehicle†	73%	8/11	4/11	3/11	2/11
KO SL 327	0%*	0/11	0/11	0/11	0/11
WT Vehicle	0%*	0/10	0/10	0/10	0/10
WT SL 327	0%*	0/10	0/10	0/10	0/10

Fisher's exact test *p < 0.03 (compared to KO Control)

†50% DMSO vehicle

Table 4

Acute mTOR inhibition does not eliminate AGS in the *Fmr1* KO

Young (P18–22) *Fmr1* KO and WT mice were injected with 6 mg/kg rapamycin or vehicle (100% DMSO). After 1 hour mice were exposed to a seizure-inducing stimulus for 2 minutes, and scored for wild running (WR), clonic seizure, tonic seizure, and death. Results reveal that treatment with rapamycin does not significantly reduce the incidence of AGS in *Fmr1* KO mice (Fisher's exact test: KO control vs. WT control *p < 0.005, KO control vs. KO rapamycin p = 0.372, KO control vs. WT rapamycin *p < 0.005). A slight decrease in AGS incidence was observed in this cohort of vehicle-treated *Fmr1* KO mice (*cf.*, Table 3), which we ascribe to the higher concentration of DMSO, required to solubilize rapamycin and ensure proper absorption.

	Incidence	Wild running	Clonic	Tonic	Death
KO Vehicle†	63%	10/16	9/16	5/16	1/16
KO rapamycin	33%	6/18	1/18	1/18	0/18
WT Vehicle	0%*	0/16	0/16	0/16	0/16
WT rapamycin	0%*	0/15	0/15	0/15	0/15

Fisher's exact test *p < 0.005 (compared to KO Control)

†100% DMSO vehicle